Molecular Psychiatry (2016) 21, 1768–1780
www.nature.com/mp

OPEN

ORIGINAL ARTICLE

A critical role for VEGF and VEGFR2 in NMDA receptor synaptic function and fear-related behavior

P De Rossi[1,2,3], E Harde[4,5,6], JP Dupuis[7,8], L Martin[1,2,3], N Chounlamountri[1,2,3], M Bardin[1,2,3], C Watrin[1,2,3], C Benetollo[1,2,9], K Pernet-Gallay[10,11], HJ Luhmann[12], J Honnorat[1,2,13], G Malleret[1,2,14], L Groc[7,8], A Acker-Palmer[4,5,6], PA Salin[1,2,14] and C Meissirel[1,2,3]

Vascular endothelial growth factor (VEGF) is known to be required for the action of antidepressant therapies but its impact on brain synaptic function is poorly characterized. Using a combination of electrophysiological, single-molecule imaging and conditional transgenic approaches, we identified the molecular basis of the VEGF effect on synaptic transmission and plasticity. VEGF increases the postsynaptic responses mediated by the *N*-methyl-D-aspartate type of glutamate receptors (GluNRs) in hippocampal neurons. This is concurrent with the formation of new synapses and with the synaptic recruitment of GluNR expressing the GluN2B subunit (GluNR-2B). VEGF induces a rapid redistribution of GluNR-2B at synaptic sites by increasing the surface dynamics of these receptors within the membrane. Consistently, silencing the expression of the VEGF receptor 2 (VEGFR2) in neural cells impairs hippocampal-dependent synaptic plasticity and consolidation of emotional memory. These findings demonstrated the direct implication of VEGF signaling in neurons via VEGFR2 in proper synaptic function. They highlight the potential of VEGF as a key regulator of GluNR synaptic function and suggest a role for VEGF in new therapeutic approaches targeting GluNR in depression.

Molecular Psychiatry (2016) **21,** 1768–1780; doi:10.1038/mp.2015.195; published online 5 January 2016

INTRODUCTION

Increasing evidence indicate that the vascular endothelial growth factor (VEGF) and its receptor VEGFR2 mediate key neurobiological processes involved in antidepressant treatment response.[1,2] These treatments, from conventional antidepressants to electroconvulsive therapies, trigger a rapid and robust increase in VEGF levels in the hippocampus in animal models.[3,4] Reciprocally, VEGF overexpression obtained *in vivo* by intracerebral administration, gene transfer or in conditional transgenic animal models, induces a VEGFR2-mediated increase in adult neurogenesis,[5–7] improves hippocampal-dependent cognition[6,8] and influences mood-related behavior with clear antidepressant effects.[9] Moreover, previous evidence documented that VEGFR2 is required for the beneficial impact of antidepressant treatments on anxiety-like behavior and anhedonia.[3,4] In contrast, endogenous VEGF depletion via small hairpin RNA silencing or inducible expression of a VEGF trap leads to altered hippocampal neurogenesis in response to enriched environment[6,10] or to selective deficits in memory.[8] Licht *et al.*[8] further demonstrated that short induction or blockade of VEGF significantly impacts on associative learning performances prior to the integration of new neurons in the hippocampal network. VEGF is able to induce rapid changes in synaptic plasticity in the dentate gyrus that could account for the gain or deficit in memory performances.[8] Yet, the underlying mechanisms responsible for the VEGF effect on hippocampal synaptic plasticity remain to be demonstrated and might shed new light on synaptic alterations linked to depression.

In the hippocampus, the NMDA type of glutamate receptor (GluNR) is a ionotropic receptor permeable for Ca^{2+} that form di and tri-heteromeric assemblies including the obligatory GluN1 subunit associated to GluN2A and/or GluN2B subunits.[11] Extensive studies have focused on the contribution of GluNR in synaptic transmission and plasticity with a specific interest for the network between CA3 and CA1 pyramidal cells in the hippocampus.[12,13] These exquisitely defined synaptic processes raise the possibility to uncover new actors that may have critical roles in regulating the efficacy of glutamatergic synaptic transmission. The regulation of synaptic strength has recently emerged as a key process implicated in the pathophysiology of depression.[14] Hence, the expression of synaptic function-related genes was reduced in prefrontal cortex of major depressive disorders subjects in link with synaptic loss.[15] Furthermore, GluNR-mediated synaptic transmission was decreased in a juvenile rat model of stress-related disorders, in association with prefrontal cortex dysfunction.[16] Thus, given the influence of VEGF on synaptic plasticity and antidepressant response, it is of interest to explore the interaction between VEGF and GluNR-mediated synaptic function. Recently, we documented a new cross-talk between VEGFR2 and GluNR that mediates the guidance of cerebellar granule neurons prior to synapse formation.[17,18] In these neurons,

[1]Institut National de la Santé et de la Recherche Médicale, Unité 1028, Centre National de la Recherche Scientifique, Unité Mixte de Recherche 5292, Lyon, France; [2]Claude Bernard University Lyon 1, Lyon, France; [3]Neurooncology and Neuroinflammation, Lyon Neuroscience Research Center, Lyon, France; [4]Institute of Cell Biology and Neuroscience and BMLS, Goethe University Frankfurt, Frankfurt, Germany; [5]Max Planck Institute for Brain Research, Frankfurt, Germany; [6]Focus Program Translational Neurosciences, University of Mainz, Mainz, Germany; [7]Interdisciplinary Institute for Neuroscience, Unité Mixte de Recherche 5297, Université de Bordeaux, Bordeaux, France; [8]Interdisciplinary Institute for Neuroscience, UMR 5297, Centre National de la Recherche Scientifique, Bordeaux, France; [9]Functional Neurogenomics and Optogenetics, Lyon Neuroscience Research Center, Lyon, France; [10]Grenoble Institute of Neurosciences, Grenoble, France; [11]INSERM U836, Microscopy and Electron Microscopy Platform, Grenoble, France; [12]Institute of Physiology, University Medical Center, University of Mainz, Mainz, Germany; [13]Neuro-Oncology Department, Hospices Civils de Lyon, Hôpital Neurologique, Lyon, France and [14]Forgetting and Cortical Dynamics, Lyon Neuroscience Research Center, Lyon, France. Correspondence: Dr C Meissirel, Equipe Neurooncologie et Neuroinflammation, Centre de Recherche en Neurosciences de Lyon, Institut National de la Santé et de la Recherche Médicale, Unité 1028, Faculté de Médecine Laennec, Lyon cedex O8, 69372 Lyon, France.
E-mail: claire.meissirel@inserm.fr
Received 21 December 2014; revised 7 October 2015; accepted 22 October 2015; published online 5 January 2016

VEGF triggers phosphorylation of GluN2B expressing GluNR (GluNR-2B) via VEGFR2, and amplify their function.[18] However, whether a VEGFR2–GluNR interaction is involved in the VEGF-dependent increase in synaptic transmission and plasticity described in hippocampal neurons, has not been explored so far.[8,19] Therefore, we hypothesized that VEGF could modulate GluNR-mediated synaptic function and plasticity in hippocampal pyramidal cells through VEGFR2. One intriguing possibility is that such a VEGF/VEGFR2-dependent mechanism might be relevant for understanding the action of new antidepressant therapies modulating GluNR function.[20]

In the present study, we identified molecular mechanisms implicated in the VEGF effect on hippocampal excitatory synaptic function, plasticity and related emotional learning processes. We first demonstrated that VEGF is able to potentiate GluNR postsynaptic responses in hippocampal pyramidal cells, via the contribution of GluNR-2B and VEGFR2. Furthermore, we showed that co-application of VEGF and NMDA to cultured hippocampal neurons induces a coordinated remodeling of GluNR-2B and α-amino-3-hydroxy-5-methyl-4-isoxazolepropionic acid (AMPA) receptor content at postsynaptic sites together with calcium–calmodulin-activated kinase (CaMKII) and protein kinase C (PKC) activation. Finally, we uncovered that VEGFR2 is required in hippocampal neurons to enable hippocampal long-term potentiation (LTP), a cellular model of memory, and consolidation of contextual fear memory.

MATERIALS AND METHODS

Animals

For experiments, wild-type P14-P15 C57Bl6J mice were used as well as two lines of transgenic mice (at P14-P15 and/or 2 months) including Nestin-cre[21] VEGFR2 conditional knockout and CaMKII-cre[22] VEGFR2 conditional knockout with related heterozygotes and control littermates. All animal experiments were conducted in accordance with the French and German institutional guidelines and ethical committees.

Culture and treatments

Primary hippocampal cell cultures were prepared from embryonic day 17 C57Bl6 mice. Low-density or high-density cultures were used after 15 days *in vitro* and left in supplemented Neurobasal medium or treated with NMDA (50 μM), VEGF (50 ng ml^{-1}) or NMDA+VEGF for 15 min prior to further processing.

Immunocytochemistry

Surface receptor expression was assayed in 15 days *in vitro* hippocampal cell cultures fixed in non-permeabilizing conditions and immunostained with antibodies recognizing the extracellular domain of corresponding proteins. After a permeabilization step, synapses were immunostained for the presynaptic synapsin-1 and/or the postsynaptic PSD95. Hippocampal pyramidal cells were subsequently imaged with Apotome microscopy (Zeiss, Jena, Germany), regions of interest were centered on apical dendrites and receptor cluster density quantified in collapsed Z-stacks.

Electrophysiology

Whole-cell patch-clamp recordings were performed in voltage-clamp mode on acute coronal hippocampal slices from non-transgenic and transgenic P14–15 pups including VEGFR2 conditional knockout and heterozygotes. Hippocampal cells were recorded in CA1 and CA3 regions and evoked GluNRs-mediated responses were isolated using gamma-aminobutyric acid type A receptor antagonist picrotoxin and AMPA-kainate receptor antagonists NBQX or CNQX in the perfusion solution. VEGF was applied locally by pressure (Picosprizer II) close to the apical dendrite of the recorded pyramidal cell (inset Figure 1b). GluNRs-mediated responses were blocked using D-2-amino-5-phosphonovalerate, MK801 and antagonists selective for GluN2B or GluN2A subunits, respectively, Ifenprodil or NVP-AAM077.

Fields recordings were performed in P30–50 acute hippocampal slices from two lines of transgenic VEGFR2 conditional mice, heterozygotes and control littermates to determine synaptic strength (input/output (I/O) curves, paired-pulse facilitation and long-term potentiation (LTP)) at the Schaffer collateral-CA1 synapses.

For VEGFR2 inhibition, hippocampal slices were treated with PTK787 (PTK), which inhibits specifically the tyrosine kinase activity of the receptor.

Single-molecule dot tracking

Quantum dots 655 coupled to goat anti-rabbit F(ab')$_2$ (Invitrogen, Carlsbad, CA, USA) were incubated on hippocampal neurons previously exposed to anti-GluN2B rabbit antibodies. Quantum dots tracking was analyzed with Metamorph software and the instantaneous diffusion coefficient calculated for each trajectory. Synaptic, perisynaptic and extrasynaptic locations for receptor/particle complex were defined with respect to MitoTracker Green labeling.

PSD fraction isolation

Postsynaptic density fractions (PSDs) were prepared as previously described[23] from treated 15 days *in vitro* hippocampal cell cultures. In brief, cells were harvested and processed for successive centrifugation steps in specific cold buffers to separate PSD from the non-PSD. PSD and non-PSD proteins were separated on sodium dodecyl sulfate-poly-acrylamide gel electrophoresis gels 4–12%, transferred on nitrocellulose membranes and immunoblotted with antibodies recognizing PSD95, synaptophysin, the GluNR subunits GluN2B and GluN2A, VEGFR2 and the GluA1 subunit of AMPA receptors. Immunoblotting of the active and total forms of CaMKII and PKCγ were also performed.

Quantification of VEGF by enzyme-linked immunosorbent assay

LTP was induced chemically (chemLTP) on acute hippocampal coronal slices from adult VEGFR2 conditional knockout and heterozygote mice, by incubating slices in tetraethylammonium chloride-containing artificial cerebrospinal fluid for 10 min. Immediately after LTP induction, VEGF levels were assessed by enzyme-linked immunosorbent assay and compared with VEGF levels in untreated conditions.

Behavior

For fear-conditioning tasks, 2-month-old-male mice including transgenic and control littermates were used. On training day, mice were placed in conditioning chamber for 2 min prior to the tone-electric footshock pairing. After 24 h, mice were tested in the training context and again 1 h later in a new context, following an exposure to the tone.

Statistics

Data are expressed as mean ± s.e.m. Distributions were tested for normality and variance equality between groups was assessed using the Levene's test. Statistical analysis were performed using as stated paired Student's *t*-tests, unpaired two-tailed *t*-tests as well as one-way analysis of variance or two-way analysis of variance. The non-parametric Kruskal–Wallis with *post hoc* tests was used when data were not normally distributed.

RESULTS

VEGF increases GluNR-mediated synaptic transmission in hippocampal neurons via VEGFR2 and postsynaptic GluNR-2B

Our goal was to determine whether VEGF might regulate glutamatergic synaptic transmission in the hippocampus. We first investigated by immunohistochemistry with validated antibodies[5,17,18,24] the spatial distribution of VEGF and its receptor VEGFR2 in P15 hippocampi. Both VEGF and VEGFR2 were expressed in the pyramidal cell layer and proximal apical dendrites in the CA1 and CA3 regions of the hippocampus (Supplementary Figure S1a–e), indicating that hippocampal pyramidal cells have the capacity to respond to endogenous VEGF.

Based on this expression pattern, we decided to study the VEGF effect on GluNR-mediated synaptic transmission in hippocampal slices from P15 animals. GluNR excitatory postsynaptic currents (EPSCs) were recorded in whole-cell patch-clamp configuration in the presence of specific gammaaminobutyric acid type A and AMPA receptor antagonists, and we compared evoked synaptic

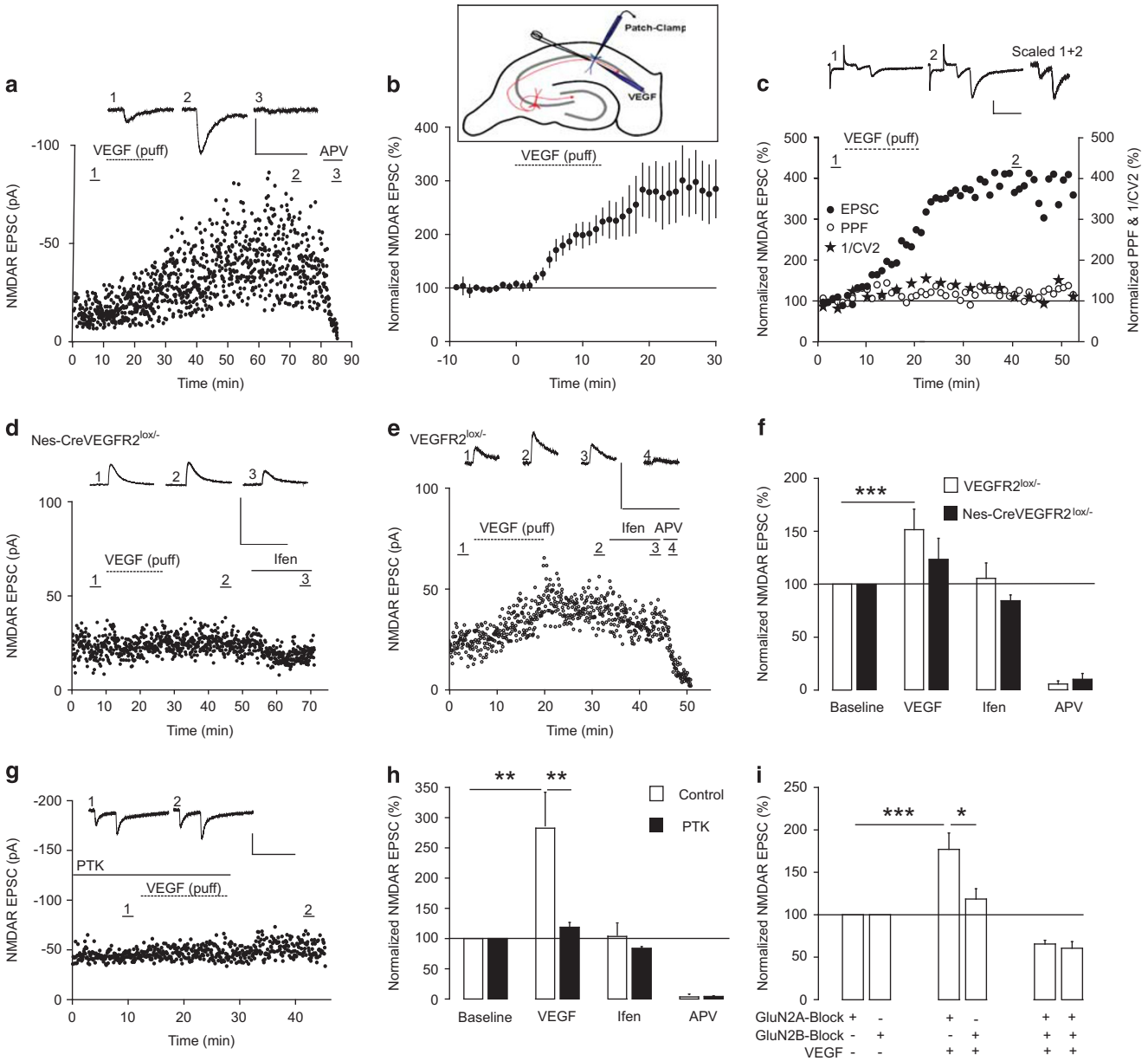

Figure 1. VEGF-dependent increase in GluNR-mediated synaptic transmission requires VEGFR2 and GluNR-2B. (**a**) Representative whole-cell patch-clamp recording of a CA1 pyramidal cell showing VEGF effect on GluNR-mediated Excitatory Postsynaptic Currents (EPSCs) at Schaffer collateral-CA1 synapses. EPSCs are illustrated in baseline condition in presence of gammaaminobutyric acid type A and AMPA receptor antagonists (1), after VEGF application (2) and APV (50 μM) (3) treatment. Note their long-term enhancement after VEGF application and their blockade with APV. (**b**) Local VEGF application showing a threefold increase in GluNR-mediated responses in CA1 ($n=8$). Inset showing VEGF topical application, local electrical stimulation of Schaffer collaterals-CA1 synapses and patch-clamp recording of a CA1 pyramidal cell. (**c**) Magnitude of PPF is characterized by PPF and inverse of the squared coefficient of variation ratios and did not change after VEGF application at Schaffer collaterals-CA1 synapses. (**d** and **e**) Representative whole-cell patch-clamp recordings showing VEGF impact on GluNR-mediated EPSCs in VEGFR2 conditional knockout mice (Nes-Cre VEGFR2$^{lox/-}$) **d** and heterozygotes (VEGFR2$^{lox/-}$) **e**. *Ifen*, (ifenprodyl, 6 μM) the NMDAR antagonist selective for GluN2B. (**f**) VEGFR2 silencing in Nes-Cre VEGFR2$^{lox/-}$ mice prevents the VEGF-dependent increase in GluNR-mediated synaptic transmission (100% of baseline and 123.3 ± 24% after VEGF, $n=6$, *P* not significant, paired Student's *t*-test) that is reported in VEGFR2$^{lox/-}$ (100% of baseline and 151.6 ± 19.3% after VEGF, $n=14$, $^{***}P<0.001$, paired Student's *t*-test). (**g**) Representative recording of synaptic responses at SC-CA1 synapses using the selective VEGFR2 inhibitor PTK787 (PTK, 30 μM). (**h**) PTK inhibited the VEGF induced enhancement of GluNR-mediated synaptic responses (100% of baseline and 118.6 ± 8.2% after VEGF, $n=6$, *P* not significant) that is reported in control condition (100% of baseline and 282.7 ± 55.5% after VEGF, $n=7$; $^{**}P<0.01$, paired Student's *t*-test; PTK versus controls: $^{**}P<0.01$). (**i**) Contribution of GluN2 subunits to normalized GluNR-mediated EPSCs was characterized with selective GluN2B and GluN2A antagonists (Ifenprodyl (6 μM) and NVP-AAM-077 (50 nM), respectively). GluN2A blockade failed to prevent the VEGF-dependent increase in GluNR-mediated synaptic responses (100% of baseline and 182.1 ± 17.3% after VEGF, $n=10$, $^{***}P<0.001$, paired Student's *t*-test) in contrast to GluN2B inhibition (100% baseline and 118.5 ± 12.1% after VEGF, $n=10$, *P* not significant, paired Student's *t*-test). Notably, the difference between the effects of GluN2B and GluN2A antagonists on VEGF-driven increase is significant ($^{*}P<0.05$). Scale bars, 50 pA, 200 ms. 1/CV^2, inverse of the squared coefficient of variation. APV, D-2-amino-5-phosphonovalerate. $^{*}P<0.05$.

responses before and after local VEGF application in CA1 or CA3. VEGF triggered a robust and long-term increase in GluNR EPSC amplitude in pyramidal cells from both CA1 (Figure 1a) and CA3 (results not shown), which was selectively blocked by the GluNR antagonist D-2-amino-5-phosphonovalerate (APV) (Figure 1a). In CA1 pyramidal cells, VEGF increased the GluNR-mediated EPSCs within 5–10 min by almost threefold (Figure 1b). To determine whether this VEGF-dependent increase in GluNR synaptic responses is due to an increase in presynaptic glutamate release probability or alternatively to a postsynaptic event, we compared the paired-pulse facilitation (PPF) obtained in baseline condition and after VEGF application. Two stimuli were applied at short intervals to induce a presynaptic facilitation of glutamate release and the PPF and the inverse of the squared coefficient of variation ratios were calculated. Changes in both ratios generally reflect an alteration in release probability but VEGF did not trigger any modification (Figure 1c), indicating a postsynaptic involvement of VEGF in the GluNR-mediated synaptic transmission.

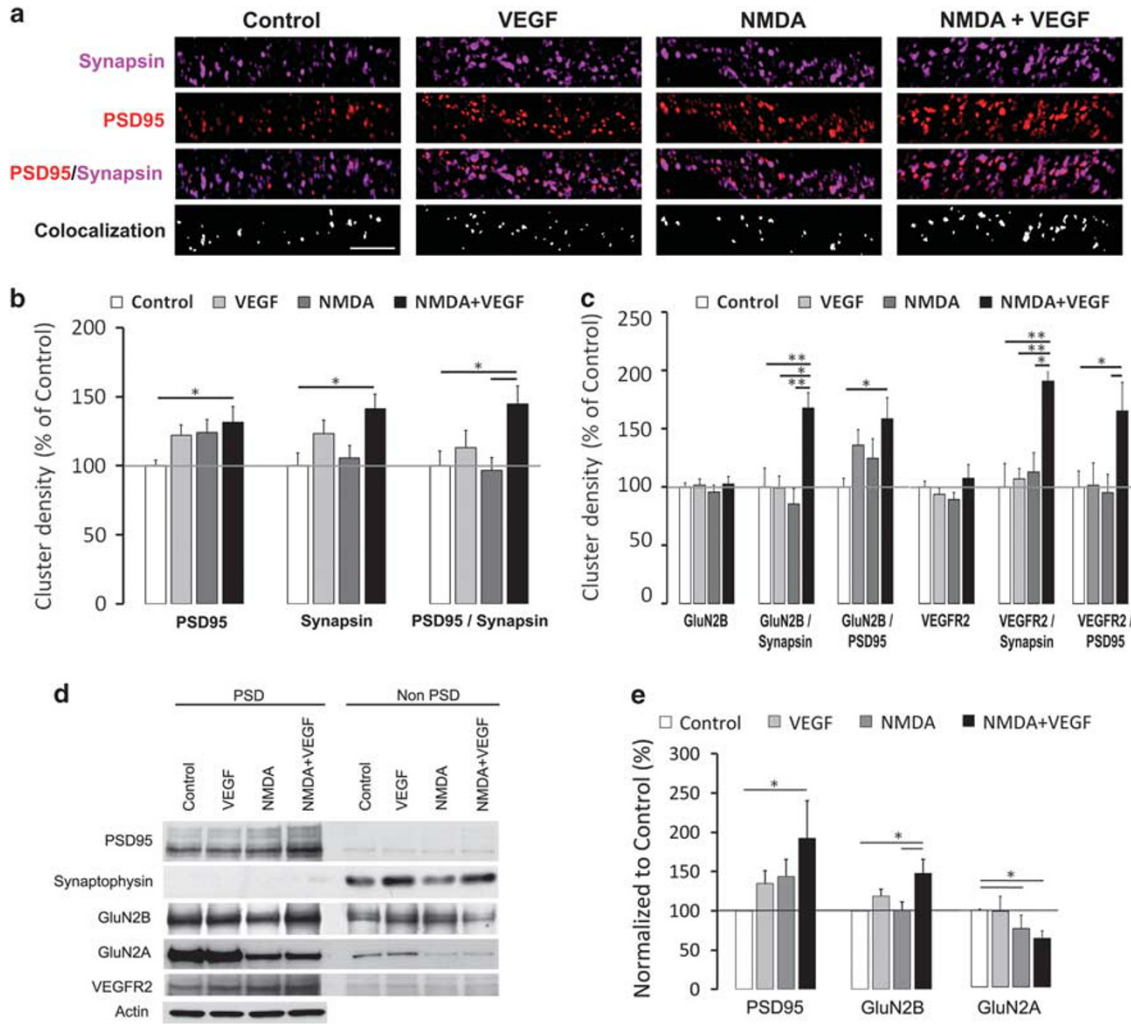

Figure 2. VEGF and NMDA-driven synapse formation and synaptic recruitment of GluNR-2B. (**a**) Representative dendritic staining in clusters for synapsin (magenta), PSD95 (red) and co-localization (white) in treated hippocampal neurons (scale bar, 5 μm). (**b**) Summary graphs showing the cluster density for PSD95, Synapsin and PSD95/Synapsin co-localization in control, VEGF, NMDA and NMDA+VEGF conditions with values normalized to control. Data were analyzed using a one-way ANOVA and when appropriate a Bonferroni *post hoc* test. Combined NMDA and VEGF application causes an increase in PSD95 and Synapsin cluster density compared with control condition (for PSD95 $100 \pm 3.9\%$ in control versus $131.3 \pm 11.3\%$ with NMDA+VEGF, $n = 25–23$, $^{*}P < 0.05$; for synapsin $100 \pm 9\%$ in control versus $141.4 \pm 10.5\%$ with NMDA+VEGF, $n = 27–18$, $^{*}P < 0.05$). Full synapses defined by co-localized PSD95 and Synapsin clusters showed an increase in density with the same treatment ($100 \pm 10.5\%$ in control versus $144.8 \pm 12.9\%$ with NMDA+VEGF, $n = 11–10$, $^{*}P < 0.05$). (**c**) Graph showing normalized values for GluN2B, VEGFR2 as well as GluN2B/synapsin, GluN2B/PSD95, VEGFR2/synapsin and VEGFR2/PSD95 cluster densities in all conditions. Data were analyzed using a one-way ANOVA and when appropriate, a Bonferroni *post hoc* test. Treatments did not affect the density of surface GluN2B and VEGFR2 clusters but their density increased significantly at synapses following NMDA and VEGF co-application as compared with control condition (for GluN2B/synapsin, with NMDA+VEGF $167.4 \pm 13.3\%$ versus control $100 \pm 16.3\%$, $n = 8–16$, $^{**}P < 0.01$; for GluN2B/PSD95, with NMDA+VEGF $158.2 \pm 17.7\%$ versus control $100 \pm 7.4\%$, $n = 12–15$, $^{*}P < 0.05$; for VEGFR2/synapsin, with NMDA+VEGF $190.9 \pm 8.1\%$ versus control $100 \pm 20\%$, $n = 8–16$, $^{**}P < 0.01$; for VEGFR2/PSD95, with NMDA+VEGF $164.8 \pm 24.7\%$ versus control $100 \pm 13.4\%$, $n = 10–15$, $^{*}P < 0.05$). Data in **b** and **c** are derived from three independent experiments. (**d**) Representative western blot of isolated postsynaptic (PSD) and non-PSD fractions from hippocampal neurons treated with control, VEGF, NMDA or NMDA+VEGF. PSD and non-PSD fractions were immunoblotted for PSD95, synaptophysin, GluN2B, GluN2A and VEGFR2. (**e**) Semi-quantitative analyses showing an increase in PSD95 and GluN2B content in PSD fractions following NMDA+VEGF treatment. All values were normalized to control. $n = 10$ independent experiments for PSD95, $n = 5$ for GluN2B and $n = 12$ for GluN2A. Data were analyzed using a Kruskal–Wallis and when appropriate a *post hoc* test. Significant differences between conditions are indicated by (*) for $P < 0.05$.

Next, we explored whether VEGFR2 mediates the VEGF-dependent effect on the postsynaptic response of pyramidal cells, using slices from genetically engineered mice. We used conditional mice expressing the Cre recombinase under the nestin promoter[21] that triggers a selective VEGFR2 deletion in neural cells (Supplementary Figure S1e and g). Whole-cell patch-clamp recordings were performed in CA1 pyramidal cells from VEGFR2 conditional knockout and heterozygote mice. Heterozygote slices display increased GluNR synaptic responses when VEGF was applied (Figure 1e and f), whereas VEGF failed to induce any significant change in GluNR EPSCs in VEGFR2 conditional knockout slices (Figure 1d and f). Thus, complete silencing of VEGFR2 in neural cells blocked the VEGF-dependent amplification of GluNR postsynaptic responses in CA1 pyramidal cells. We further assessed whether pharmacological blockade of VEGFR2 would support our genetic findings. Application of PTK787, a blocker that specifically inhibits the tyrosine kinase activity of VEGFR2, neutralized the amplifying effect of VEGF (Figure 1g and h). Overall, these electrophysiological findings provide strong evidence that VEGF effect on GluNR-mediated synaptic responses acts through VEGFR2.

To gain insight into the GluNR subunit involved in this VEGF induced effect, we examined GluNR postsynaptic responses in hippocampal slices treated with GluN2B or GluN2A selective antagonists (ifenprodyl and NVP-AAM077,[25] respectively). With ifenprodyl treatment, VEGF failed to induce a significant increase in GluNR EPSCs, whereas NVP-AAM077 had no significant effect and did not prevent the VEGF-dependent increase in synaptic responses (Figure 1i). Thus, our data indicate that GluN2B expressing GluNR (GluNR-2B) mediate the VEGF-dependent increase in evoked postsynaptic responses in hippocampal neurons.

VEGF and GluNR receptor co-activation promotes synapse formation and accumulation of GluNR-2B at synapses

Postsynaptic mechanisms underlying the VEGF-dependent increase in GluNR synaptic transmission may involve an increase in GluNR-2B synaptic expression and/or a change in receptor function. To test whether VEGF is able to recruit GluNR-2B to synaptic sites, we stimulated the total pool of GluNR and/or VEGFR2 in cultured hippocampal neurons with bath applications of NMDA and/or VEGF.[19,26] These short treatments did not cause major toxic effects with NMDA and failed to increase cell viability with VEGF, as assessed using Live/dead assay and western blotting (Supplementary Figure S2). Only high doses of NMDA downregulated activation of the pro-survival extracellular signal-regulated kinase 1/2 and activated the pro-death molecule caspase-3 (Supplementary Figure S2f).

To determine the impact of VEGF on synaptic expression of VEGFR2 and GluNR-2B in hippocampal neurons, we quantified the cluster density of cell surface receptors in apical dendrites of non-permeabilized fixed pyramidal cells. Synaptic sites were identified with the commonly used presynaptic vesicle marker synapsin-1 and/or the postsynaptic density marker PSD95 (Figure 2a). Quantitative analysis of synaptic sites, identified as PSD95 or synapsin-1 clusters, and full synapses (PSD95 and synapsin-1 co-clusters) indicated that their density was only increased with combined NMDA and VEGF treatment compared with control (Figure 2a and b). To investigate whether this increase in synaptic site density was associated with morphological changes of dendritic spines and synapses, we respectively used confocal and electron microscopy on treated hippocampal neurons. The quantitative confocal imaging of enhanced green fluorescent protein-expressing neurons showed that NMDA and VEGF combined stimulation selectively promoted the formation of new dendritic spines (Supplementary Figure S3a–c). This emergence of new dendritic protrusions resulted in part from the appearance of *de novo* spines, as revealed by time-lapse imaging (Supplementary Figure S3d). In addition, dynamic changes in spine morphology were also detected with an increase in spine head size induced by NMDA and VEGF treatment (Supplementary Figure S3d). Electron microscopic analyses further documented a significant increase in PSD length under VEGF and combined NMDA and VEGF treatments, in link with an occurrence of perforated synapses (Supplementary Figure S4a–e). However, only the combined NMDA and VEGF condition triggered a major PSD remodeling with a concurrent enhancement of PSD length and thickness (Supplementary Figure S4e). Thus, our data demonstrated that new synaptic sites are induced after brief NMDA and VEGF exposure through dendritic spine formation and PSD remodeling.

None of the applied treatments did affect the global expression of surface GluNR-2B (identified by immunostaining of their GluN2B subunit) or VEGFR2 in dendrites (Figure 2c and Supplementary Figure S5). In contrast, their synaptic location characterized by the density of GluN2B/synapsin or GluN2B/PSD95 co-clusters and VEGFR2/synapsin or VEGFR2/PSD95 co-clusters was significantly enhanced with NMDA and VEGF co-application compared with control condition (Figure 2c and Supplementary Figure S5). Together, our findings demonstrate that the co-activation of NMDA and VEGF receptors in hippocampal pyramidal neurons

Figure 3. Increase in GluNR-2B surface diffusion and synaptic accumulation induced by VEGF and NMDA. (**a**) Cumulative distributions of the instantaneous diffusion coefficients of synaptic GluNR-2B before (Control, black) and after buffer, VEGF, NMDA or VEGF+NMDA (gray) administration. The first point of each distribution corresponds to the fraction of immobile receptors (diffusion coefficient $< 0.005\ \mu m^2\ s^{-1}$). Kolmogorov–Smirnov test on cumulative distributions: control versus buffer, *P* not significant; control versus VEGF, $P < 0.0001$; control versus NMDA, $P < 0.0001$; control versus VEGF+NMDA, $P < 0.0001$. (**b**) Representative trajectories (500 frames, 20-Hz acquisition rate) of surface GluNR-2B (scale bar, 1 μm) after Buffer, VEGF, NMDA or VEGF+NMDA administration. Gray, synaptic area (syn.). (**c**) Normalized instantaneous diffusion coefficients of synaptic GluNR-2B (mean ± s.e.m.) before (Control, white bars) and after Buffer, VEGF, NMDA or VEGF+NMDA (gray bars) administration (example 6–10 min after treatment: control 100 ± 3.9%, $n = 919$ trajectories, versus buffer 101.9 ± 4.7%, $n = 618$, *P* non-significant; control 100 ± 3.8%, $n = 742$, versus VEGF 89.1 ± 5.3%, $n = 355$, $^*P < 0.05$; control 100 ± 4.5%, $n = 529$, versus NMDA 72.0 ± 3.8%, $n = 542$, $^{***}P < 0.0001$; control 100 ± 4.5%, $n = 712$, versus VEGF+NMDA 126.5 ± 6.3%, $n = 460$, $^{***}P < 0.0001$). (**d**) Representative surface distributions of single GluNR-2B in the synaptic area (gray, syn.) during a standard acquisition (500 frames, 20-Hz acquisition rate) after Buffer, VEGF, NMDA or VEGF+NMDA administration. Each blue dot represents the detection of a single receptor during a frame (scale bar, 400 nm). (**e**) Normalized GluNR-2B synaptic dwell time (mean ± s.e.m.) before (control, white bars) and after Buffer, VEGF, NMDA or VEGF+NMDA (gray bars) administration (example 11–15 min after treatment: control 100 ± 2.6% versus buffer 103 ± 5%, *P* non-significant; control 100 ± 2.6% versus VEGF 98.3 ± 5.4%, *P* non-significant; control 100 ± 2.6% versus NMDA 102.9 ± 5.9%, *P* non-significant; control 100 ± 2.6% versus VEGF+NMDA 115.1 ± 7.7%, $^*P < 0.05$). (**f**) Normalized synaptic fraction of detected GluNR-2B (mean ± s.e.m.) before (control, white bars) and after Buffer, VEGF, NMDA or VEGF+NMDA (gray bars) administration. No change in GluNR-2B synaptic content was observed after 11–15 min administration of buffer, VEGF or NMDA alone (control 100 ± 4.3%, $n = 10$ neuronal fields versus VEGF 96.1 ± 8.2%, $n = 8$, *P* not significant; control 100 ± 8%, $n = 9$ versus NMDA 107.8 ± 5.1%, $n = 9$, *P* not significant). However, GluNR-2B synaptic fraction was increased following 11–15 min of VEGF+NMDA compared with control (control 100 ± 6.2%, $n = 9$ versus VEGF+NMDA 126.3 ± 8.2%, $n = 9$, $^*P < 0.05$). Comparison between groups for instantaneous diffusion coefficients, normalized synaptic dwell time and synaptic fraction were analyzed using a Kruskal–Wallis and *post hoc* Dunn's test.

triggers synaptogenesis and promotes the synaptic targeting of GluNR-2B and VEGFR2.

To confirm this synaptic targeting process, we isolated the postsynaptic density fractions (PSDs) from treated hippocampal neurons and analyzed the expression of the GluN2 subunits GluN2B and GluN2A, and of VEGFR2 and PSD95 by immunoblotting. The resulting enrichment of PSD95 in PSDs and of the presynaptic protein synaptophysin in non-PSD fractions validated the purification protocol (Figure 2d). Our biochemical findings revealed that combined NMDA and VEGF treatment is able to

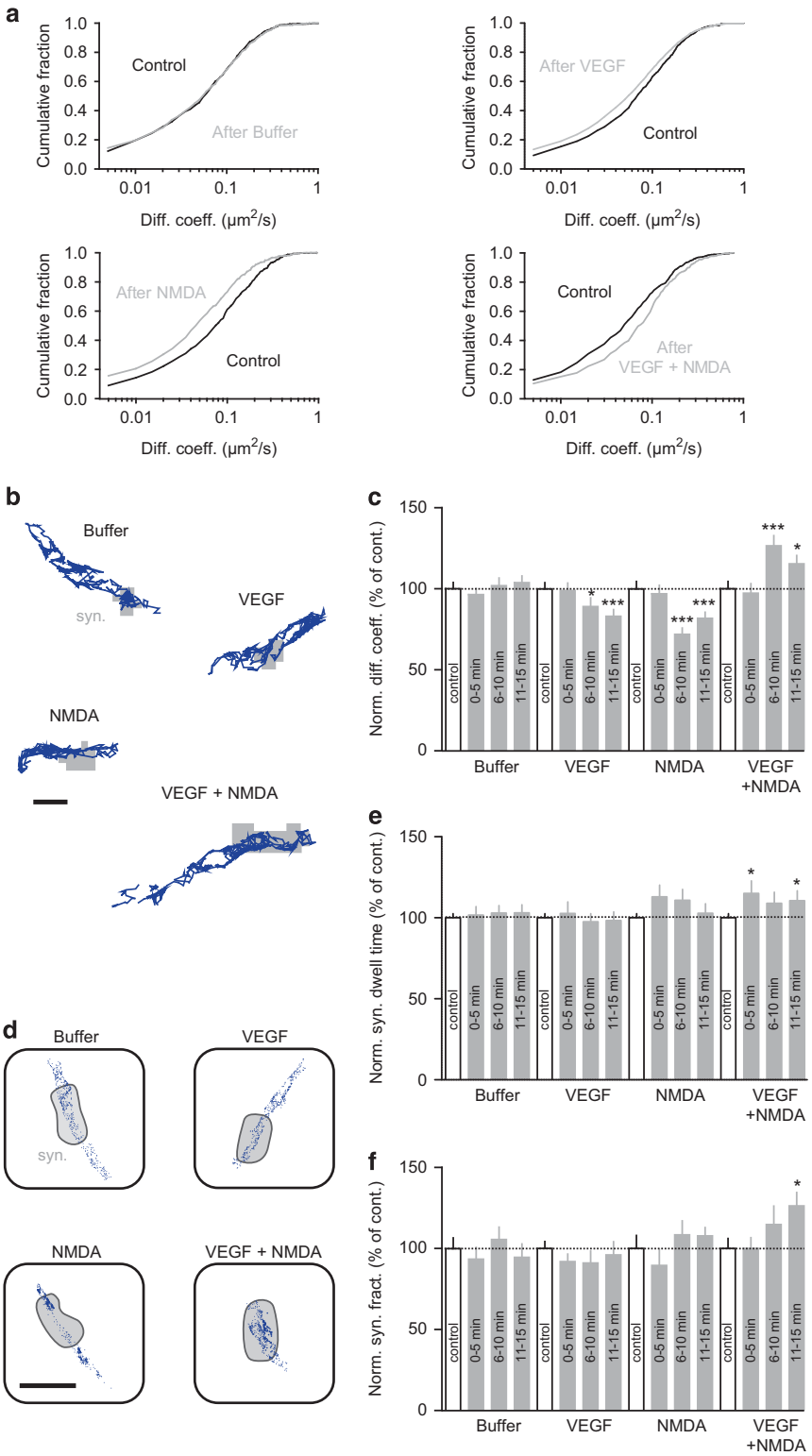

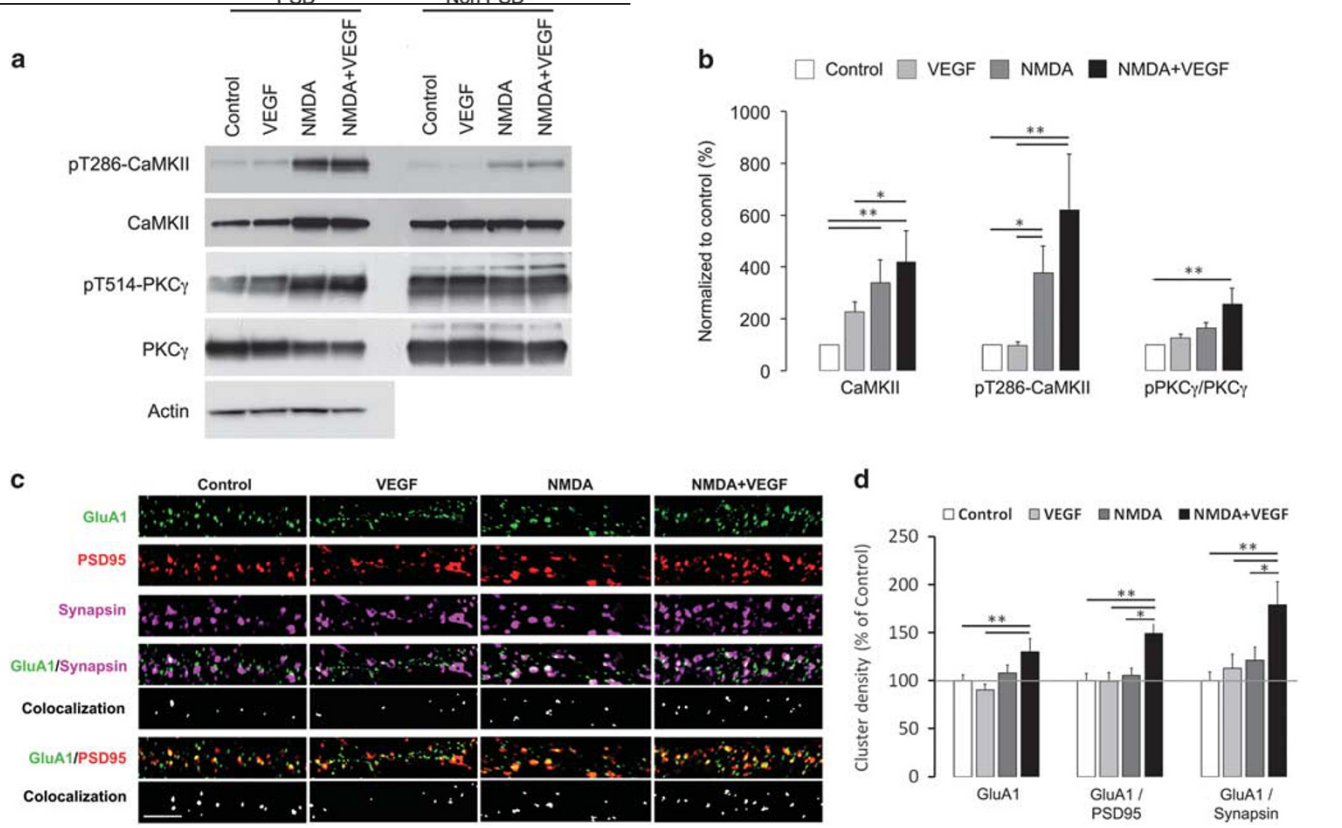

Figure 4. VEGF and NMDA administration induced signaling pathways and AMPAR synaptic delivery in hippocampal neurons. (**a**) Immunoblots of total and phosphorylated forms of CaMKII and PKCγ in PSDs upon treatments. PSD and non-PSD fractions were purified from hippocampal cultures exposed to control, VEGF, NMDA and NMDA+VEGF. (**b**) Analysis of protein expression levels normalized to control showing the increase in total and active CaMKII (pT286-CaMKII) induced by NMDA and NMDA+VEGF treatments compared with control, which reflects the translocation of these two forms of CaMKII to PSD. Note that the phosphorylated to total PKCγ ratio was also significantly increased in PSDs upon exposition to NMDA+VEGF compared with control. Respectively $n=9$ independent experiments for CaMKII and $n=7$ for PKCγ; significant differences between conditions were determined using a Kruskal–Wallis with a *post hoc* test and are indicated by (*) for $P<0.05$; (**) for $P<0.01$. (**c**) Representative dendritic immunostaining in clusters for GluA1 (green), PSD95 (red) and synapsin (magenta), as well as for GluA1/synapsin and GluA1/PSD95 co-localization (white) (scale bar, 5 μm). (**d**) Graphs showing the density of GluA1 clusters, respectively, at the dendritic surface and at synaptic sites defined by PSD95 or synapsin labeling. Values were normalized to control and analyzed using a one-way ANOVA and when appropriate a Bonferroni *post hoc* test. Following NMDA and VEGF treatment, surface GluA1 clusters increased in density compared with control and VEGF alone (with NMDA+VEGF $130\pm13.8\%$ versus control $100\pm6.1\%$, $n=10$–11, $^{**}P<0.01$; versus VEGF $90.2\pm6.2\%$, $n=10$–15, $^{**}P<0.01$) and accumulated at synapses compared with the other conditions (for PSD95 labeled synapses: with NMDA+VEGF $148.9\pm14.6\%$ versus control $100\pm7.4\%$, $n=10$–11, $^{**}P<0.01$; versus VEGF $99\pm9.7\%$, $n=10$–15, $^{**}P<0.01$; versus NMDA $105.5\pm7.3\%$, $n=10$–15, $^{*}P<0.05$). Data shown are derived from three independent experiments.

increase the expression level of PSD95 and GluN2B in PSDs compared with control (Figure 2d and e). In contrast, we observed an opposite trend toward a decrease in the level of GluN2A expressed in PSDs with the same treatment (Figure 2d and e). These data further provide the first evidence that VEGFR2 is located at the PSDs in hippocampal neurons (Figure 2d), and therefore supports the contribution of this vascular receptor in the regulation of synaptic transmission through postsynaptic mechanisms. Thus, we confirmed the postsynaptic enrichment in GluNR-2B when NMDA and VEGF receptors are co-activated, in agreement with the VEGF-dependent increase in evoked postsynaptic responses in hippocampal slices.

Postsynaptic accumulation of GluNR-2B results from an increase in surface diffusion

Growing evidence indicate that the regulation of synaptic content in receptors depends on their surface-trafficking properties.[27] Thus, we used the single nanoparticle-tracking approach (quantum dots)[28] to further investigate whether application of NMDA, VEGF or NMDA in combination with VEGF impacted the surface diffusion and distribution of GluNR-2B receptors in cultured hippocampal neurons. Buffer additions did not affect the diffusion of GluNR-2B, whereas exposure to NMDA or VEGF alone slowed down the surface mobility of synaptic receptors (Figure 3a–c). However, none of these treatments affected the synaptic content in GluNR-2B (Figure 3d and f). In contrast, combining NMDA and VEGF induced a significant increase in the diffusion of GluNR-2B (Figure 3a–c). This change likely relied on an upregulation of GluNR-2B diffusion properties rather than on an increase in the fraction of mobile receptors (diffusion coefficient $>0.005\ \mu m^2\ s^{-1}$; control, 87.1% of mobile GluNR-2B; VEGF +NMDA, 89.6% of mobile GluNR-2B), as attested by the cumulative distributions of diffusion coefficients (Figure 3a). Moreover, this increased surface diffusion of GluNR-2B, associated with an increase in synaptic dwell time (Figure 3e), resulted in the accumulation of receptors at synapses (Figure 3d and f). Thus, by promoting an increase in surface diffusion of GluNR-2B, the co-activation of NMDA and VEGF receptors triggers GluNR-2B redistribution and accumulation at synapses.

VEGF and NMDA-driven signaling pathways

To characterize the molecular mechanisms underlying the synaptic targeting of GluNR-2B, we investigated downstream signaling pathways activated at the PSD by the co-application of

NMDA and VEGF. Given the key role of CaMKII in the postsynaptic expression and surface dynamics of GluNR-2B,[29–31] we analyzed the expression and activation of the kinase in PSDs purified from treated hippocampal cultures. Our biochemical data confirmed that GluNR activation is instrumental for the autophosphorylation of CaMKII and its translocation to PSD (Figure 4a and b), as previously shown.[32] Combined NMDA and VEGF treatment did not show any further increase in the CaMKII phosphorylation levels and the presence of CaMKII at the PSD (Figure 4a and b).

Protein kinase C (PKC) also has a critical role in the regulation of GluNR trafficking by triggering their rapid insertion into the plasma membrane in hippocampal neurons and Xenopus oocytes-expressing recombinant GluNRs.[33–35] Therefore, we isolated PSD fractions derived from treated hippocampal cultures and immunoblotted them for the total PKCγ levels and its phosphorylated (T514) form, required for PKCγ maturation and rate-limiting for its activation.[36] Analysis of the phosphorylated to native PKCγ ratio revealed a significant increase following the combined NMDA and VEGF stimulation compared with control conditions, indicating an accumulation of catalytically competent PKCγ at the PSDs (Figure 4a and b). Thus, the acute co-activation of NMDA and VEGF receptors induces a concomitant increase in autonomously active CaMKII and PKCγ at PSD, which is tightly associated with the enrichment of GluNR-2B at synaptic sites.

Synaptic incorporation of AMPA receptors upon co-activation of VEGF and GluNR receptors

Activation of PKC and CaMKII signaling pathways is known to independently increase recruitment of GluA1-expressing AMPA receptors (GluA1-AMPAR) to synapses.[37–39] Given the activation of CaMKII and PKC upon NMDA and VEGF stimulation, we further explored whether this stimulation protocol was also able to promote an enrichment of AMPA receptors at synaptic sites. Thus, we performed a GluA1 surface immunostaining in combination with a selective labeling of synaptic sites in hippocampal neurons. We showed an increase in density of surface GluA1 clusters following the NMDA and VEGF treatment compared with the control condition and the stimulation with VEGF alone (Figure 4c and d). These data strongly suggest an insertion of new GluA1-AMPAR into the plasma membrane and a stabilization of the surface receptors already present. To determine whether this increased pool of surface GluA1-AMPAR was targeted to synapses, we quantified the co-localization of PSD95 or synapsin-1 with GluA1 clusters. Our results revealed an increased amount of surface GluA1 at synaptic sites upon co-activation of NMDA and VEGF receptors compared with the other conditions (Figure 4d). Altogether, our findings demonstrate that molecular mechanisms known to be involved in LTP, such as PKC and CaMKII activation and AMPAR synaptic insertion,[35,40] are triggered by VEGF when GluNR are activated.

VEGFR2 conditional knockout mice show impaired hippocampal LTP and fear memory consolidation

The involvement of VEGF in mechanisms underlying LTP raised the possibility that neuronal VEGFR2 may regulate the magnitude of LTP in the hippocampus. A prerequisite for a modulatory action of VEGFR2 during LTP is the availability of VEGF in the neuronal microenvironment. To evaluate this availability, we analyzed endogenous VEGF secretion in acute hippocampal slices from P30–50 old mice with a conditional deletion of VEGFR2 in neural cells, or heterozygous for the VEGFR2 allele, following chemically induced LTP with tetraethylammonium chloride (chemLTP). Levels of VEGF released in the slice microenvironment, which represent the functional fraction, were compared between untreated and tetraethylammonium chloride-treated slices with enzyme-linked immunosorbent assay measurements. Our findings demonstrate an increase in endogenous VEGF release in response to chemLTP stimulation in both genotypes (Figure 5a). Thus, critical levels of VEGF might be required in the process of LTP.

Next, to explore the role of VEGFR2, we assessed LTP induced by theta burst stimulation of Schaffer collaterals/commissural afferents in CA1 (SC-CA1 synapses) from knockout, heterozygotes and littermates control hippocampal slices. Although LTP was induced under theta burst stimulation in all groups (Figure 5b), the mean fEPSP slope was significantly reduced as soon as 5 min after theta burst stimulation and remained altered 55–60 min after theta burst stimulation in VEGFR2ko mice compared with heterozygotes and control mice (Figure 5b–d). LTP impairments in knockout mice were not due to an alteration in basal synaptic transmission or presynaptic release probability, as we observed no significant differences among the groups in the input output curve (I/O curve) (Figure 5e) and in measurements of PPF (Figure 5f). Consistent with these findings, similar defective LTP was also observed when the tyrosine kinase activity of VEGFR2 was pharmacologically inhibited using PTK787 in control hippocampal slices (Figure 5g–i).

To further assess the relevance of VEGFR2 in LTP induction, we examined the impact of a VEGFR2 deletion specifically in postmitotic neurons of the forebrain using the αCaMKII-Cre transgene to generate conditional VEGFR2ko mice. We first investigated the VEGFR2 immunolabeling pattern in these CaMKII-Cre-floxed mice and validated the loss of neuronal VEGFR2 in the hippocampus (Supplementary Figure S1f). Next, our electrophysiological data confirmed that deletion of VEGFR2 in hippocampal neurons triggers a deficit in SC-CA1 LTP without affecting basal synaptic transmission (Supplementary Figure S6). Overall, our findings demonstrated a requirement for VEGFR2 expression in hippocampal neurons to induce normal LTP.

Finally, we examined whether this alteration in hippocampal LTP impacted on hippocampal-dependent emotional memory by studying contextual fear learning. We used a cued fear-conditioning procedure, which allows assessment of both contextual fear learning relying on hippocampus and amygdala functions and cued fear learning, which is only amygdala-dependent. Because amygdala is critically involved in emotion and anxiety in both tests, we first confirmed the neuronal expression of VEGFR2 in this structure in control mice (Supplementary Figure 7a and b). During conditioning, all groups of mice showed a robust increase in freezing time in response to a tone-electrical shock pairing, compared with the period prior to the pairing, and no differences were detected between genotypes (Figure 5j). When tested 24 h later in the same context without tone-electrical shock pairing, VEGFR2ko mice were impaired on this task compared with control and heterozygote mice and spent significantly less time freezing (Figure 5k). In the cued test assessed in a new context with the auditory cue alone, the freezing behavior was increased during the tone for all groups of mice, but VEGFR2ko mice showed again a large reduction in freezing time compared with control and heterozygote mice (Figure 5l). Importantly, the decrease in freezing behavior of VEGFR2ko mice during contextual and cued tests demonstrated that the formation of contextual and cued fear memory is impaired in these mice. Thus, both the amygdala and hippocampal functions might be affected in mice by the loss of VEGFR2 in neural cells.

DISCUSSION

This study demonstrates for the first time that VEGFR2 is required for hippocampal synaptic plasticity and related fear memory and uncovers underlying mechanisms linked to the impact of VEGF on GluNR-mediated synaptic transmission. Based on a combination of single-molecule imaging, biochemical, electrophysiological and behavioral approaches, we have analyzed the synaptic basis of the VEGF action on hippocampal neurons and its contribution to synaptic plasticity and fear memory. Our analysis first shows

that the expression pattern of both VEGF and its receptor VEGFR2 is complementary in the CA1 and CA3 regions of the hippocampus, consistent with a role for VEGF/VEGFR2 in hippocampal networks. Second, we report a rapid increase in GluNR-mediated currents induced by VEGF in hippocampal neurons that requires the postsynaptic contribution of GluNR-2B. Further evidence indicates that VEGF triggers the formation of synapses and promotes the surface dynamics and synaptic accumulation of GluNR-2B when NMDA receptors are activated. This enrichment in synaptic GluNR-2B occurs concurrently with an increase in CaMKII and

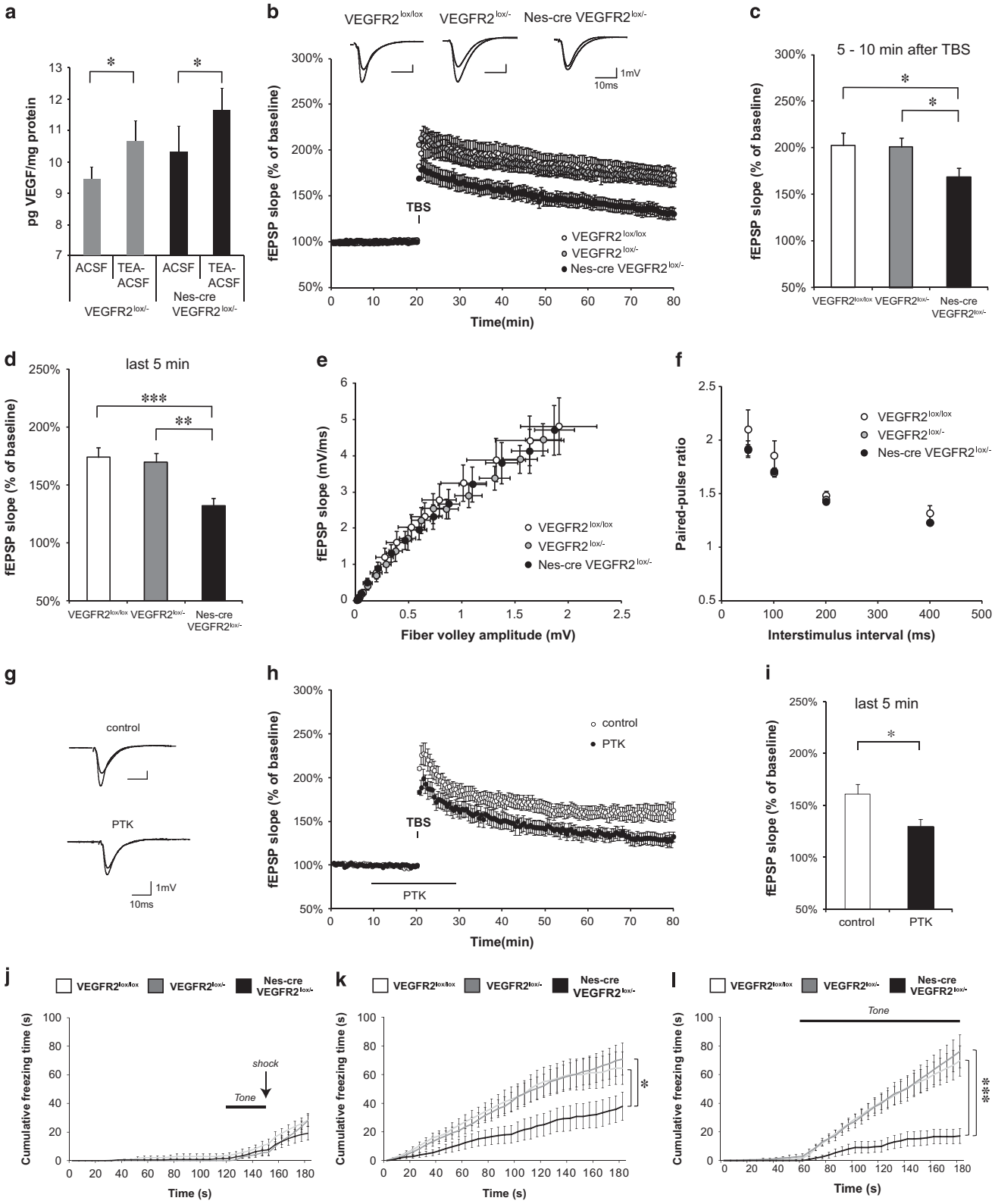

PKC activation in PSDs. Finally, using conditional invalidation mice models, we have uncovered the requirement for VEGFR2 in hippocampal LTP and consolidation of fear memory.

In a recent study, we documented a VEGF/GluNR link in cerebellar neuronal guidance before synapse formation occurs.[18] The interaction between VEGFR2 and GluNR raised questions about a putative regulatory function that VEGFR2 could have on GluNR dependent neurotransmission. Previous studies have reported that VEGF can regulate the activity of ion channels in endothelial and heterologous cells[41,42] as well as in hippocampal neurons.[43,44] VEGF has been shown to either suppress or increase evoked excitatory synaptic transmission in the hippocampus in different contexts.[19,45,46] Hippocampal synaptic responses to VEGF obtained in adult rodent hippocampal slices differed depending on the concentration and kinetic of the VEGF delivery. Short-term exposure to low doses of VEGF induced a potentiation of synaptic responses,[19] whereas high doses of VEGF applied for a longer period of time resulted in a depression of synaptic transmission.[45,46] These studies raised intriguing questions about indirect effects of VEGF on neurons involving endothelial or glial cells, which may explain why VEGF can induce opposite changes in synaptic responses. To minimize indirect effects, we investigated the impact of a brief topical application of VEGF on GluNR-mediated synaptic transmission in hippocampal pyramidal cells. VEGF triggered a rapid increase in postsynaptic GluNR currents that requires VEGFR2 expression in hippocampal pyramidal cells, as evidenced by the effect of VEGFR2 pharmacological inhibition and by our results in the neural-specific VEGFR2 conditional knockout. Indirect effects via astrocytes are unlikely because these cells express prominently VEGFR1.[47] However, we cannot exclude a contribution of the VEGFR2 co-receptors Neuropilin-1 and Neuropilin-2 that have been previously documented to be expressed in hippocampal dendrites and synapses.[48–50] Consistently, we found that VEGFR2 is localized primarily on the proximal apical dendrite of hippocampal pyramidal cells, at the postsynaptic densities of excitatory synapses, together with GluNR-2B and the PSD95 scaffolding protein. Notably, the contribution of GluNR-2B to synaptic responses of CA1 pyramidal cells has been shown to be higher for Schaffer collaterals inputs onto proximal dendrites than for the perforant path on distal dendrites.[51]

Overall our findings demonstrate that the convergence between VEGF signal and glutamatergic inputs has a key role at hippocampal excitatory synapses in enhancing transmission mediated by GluNR.

The synaptic changes described in this study require a VEGF-dependent increase in targeting of GluNR at synapses. Increasing evidence indicate that synaptic composition of GluNR changes during postnatal development in many brain regions with a progressive decrease in the GluN2B/GluN2A subunit ratio.[11,52,53] In 15 days *in vitro* cultured hippocampal neurons, only 21% of GluNR-2B are located at synapses with a shorter residency time compared with GluNR-2A.[52] Thus, GluNR-2A could be good candidates for mediating the VEGF-dependent effect on synaptic responses; however, our electrophysiological work demonstrates that in fact GluNR-2B are the major contributor to the postsynaptic effects. We further investigated the underlying mechanism and documented a VEGF and NMDA-driven enrichment in synaptic GluNR-2B and PSD95, combined with the formation of new synaptic sites in hippocampal pyramidal cells.

Our findings are consistent with previous reports suggesting a causal link between synaptic GluNR-2B and synapse formation and plasticity during development.[54,55] These studies used genetic manipulations designed to overexpress GluN2A, or replace GluN2B into GluN2A, and pointed to the key role of GluNR-2B in hippocampal synaptogenesis and synaptic plasticity, as well as in expression of normal social behavior.[54–57] This raises the question of how VEGF might trigger such a mobilization of GluNR-2B at synapses. GluNR-2B insertion at synapses is known to be constitutive and independent of glutamatergic synaptic activity,[58]

Figure 5. Hippocampal LTP as well as contextual and cued fear memory are impaired in VEGFR2 conditional knockout mice and upon VEGFR2 inhibition. The three genotypes include control mice or $VEGFR2^{lox/lox}$, heterozygotes or $VEGFR2^{lox/-}$ and conditional VEGFR2 knockout mice or Nes-cre $VEGFR2^{lox/-}$. (**a**) VEGF levels, assessed by Elisa, increased upon chemical LTP induction (tetraethylammonium chloride-artificial cerebrospinal fluid) compared with untreated condition (artificial cerebrospinal fluid) in both heterozygote and knockout adult hippocampal slices (pg VEGF per mg protein from 9.4 ± 0.4 to 10.7 ± 0.7 in $VEGFR2^{lox/-}$ slices, $n = 7$, paired two-tailed *t*-test, $^*P < 0.05$; from 10.3 ± 0.8 to 11.7 ± 0.7 in Nes-cre $VEGFR2^{lox/-}$ slices, $n = 8$, paired two-tailed *t*-test, $^*P < 0.05$). (**b**) Representative fEPSP traces showing potentiation for the three indicated genotypes (upper trace: averaged first 5 min of baseline, lower trace: averaged last 5 min, stimulus artifacts were removed). Theta burst stimulation (TBS) of Schaffer collaterals was used to induce LTP and fEPSP responses were recorded in stratum radiatum of CA1 region. (Nes-cre $VEGFR2^{lox/-}$ $n = 11$ mice (25 slices), $VEGFR2^{lox/-}$ $n = 17$ mice (36 slices), $VEGFR2^{lox/lox}$ $n = 8$ mice (15 slices). (**c**) Shortly (5–10 min) after LTP induction with the TBS protocol the fEPSP was significantly reduced in Nestin-cre $VEGFR2^{lox/-}$ knockout mice compared with heterozygotes and controls ($169 \pm 9\%$ in Nes-cre $VEGFR2^{lox/-}$ versus $201 \pm 10\%$ in $VEGFR2^{lox/-}$ and $203 \pm 14\%$ in $VEGFR2^{lox/lox}$, unpaired two-tailed *t*-test, $^*P < 0.05$). (**d**) An even more pronounced reduction in LTP was observed at 55–60 min after TBS ($132 \pm 6\%$ in Nes-cre $VEGFR2^{lox/-}$ versus $169 \pm 8\%$ in $VEGFR2^{lox/-}$ and $174 \pm 9\%$ in $VEGFR2^{lox/lox}$, unpaired two-tailed *t*-test, $^{**}P < 0.01$, $^{***}P < 0.001$). (**e**) Input–output curves showing fEPSP slopes at different stimulation intensities (fiber volley amplitude). The three groups of mice showed no significant differences. (**f**) VEGFR2 knockout slices showed normal paired-pulse facilitation at various interstimulus intervals (50, 100, 200 and 400 ms). No significant differences were obtained among the three genotypes. (**g**–**i**) VEGFR2 inhibition in hippocampal LTP. (**g**) Representative fEPSP traces showing potentiation for wild-type slices untreated and treated with 30 μM PTK787 (upper trace: averaged first 5 min of baseline, lower trace: averaged last 5 min, stimulus artifacts were removed). (**h**) LTP was induced by TBS stimulation of Schaffer collaterals and fEPSP responses were recorded in stratum radiatum of CA1 region. Hippocampal slices were perfused with 30 μM of the VEGFR2 inhibitor PTK787 (PTK) from 10 min before until 10 min after LTP induction (control $n = 7$ mice (11 slices), PTK $n = 4$ mice (7 slices)). (**i**) LTP magnitude was significantly reduced 55–60 min after TBS in slices treated with PTK ($161 \pm 10\%$ in control slices vs $130 \pm 7\%$ in PTK treated slices, unpaired two-tailed *t*-test, $^*P < 0.05$). (**j**–**l**) Fear-conditioning experiment. Animals were placed in a context and presented with an electrical shock (arrow) paired once with an auditory cue (Tone); data were analyzed using a two-way ANOVA (genotype, time) with $n = 12$ per genotype. (**j**) Cumulative freezing time counted during the 3-min conditioning period. There were no significant differences between genotype ($F(2,33) = 1.27$; *P* not significant) and all genotypes showed a progressive increase in freezing after the Tone-shock pairing. (**k**) Cumulative freezing time plotted over time during the 3 min of the context recognition test. There was a significant effect of genotype ($F(2,33) = 3.30$; $^*P < 0.05$) and Nes-cre $VEGFR2^{lox/-}$ knockout mice showed reduced freezing time compared with heterozygotes and controls ($^*P < 0.05$, Bonferroni *post hoc* test). (**l**) Cumulative freezing time during cued testing. There was a significant effect of genotype ($F(2,33) = 9,59$; $^{***}P < 0.001$) and only controls and heterozygotes showed a major increase in freezing time during the tone presentation as compared with prior to the tone. Nes-cre $VEGFR2^{lox/-}$ knockout mice exhibited strongly reduced level of freezing compared with heterozygotes and controls ($^{***}P < 0.001$, Bonferroni *post hoc* test). ACSF, artificial cerebrospinal fluid; TEA, tetraethylammonium chloride.

but their synaptic trafficking can be promoted through PKC-dependent signaling mechanisms.[34] We demonstrated that PKC is involved in the action of VEGF when GluNR are activated, which is consistent with the well-known impact of this kinase on GluNR trafficking and synaptic responses.[33,34]

The synaptic pool of GluNR is also regulated by the lateral diffusion of these receptors within the membrane between synaptic and extrasynaptic sites.[52,59] The ability of GluNR to rapidly move between these compartments is linked to their subunit composition, because GluN2B containing GluNR are the most mobile,[52] and their lateral diffusion can be increased by synaptic plasticity in young hippocampal neurons.[31] The activity-driven diffusion of surface GluNR results in an enrichment of GluNR-2A at synapses, whereas GluNR-2B are displaced away from the synapse.[31,60] Reciprocally, our study demonstrates that VEGF, when combined to NMDA, induces an increase in surface dynamics of GluNR-2B, which leads to their enrichment at synapses. Importantly, this VEGF-dependent mobilization of GluNR-2B at synapses may increase calcium concentration in spines, allowing the modulation of synaptic plasticity.

A major form of synapse strengthening known as LTP critically depends on GluNR-mediated activation in the CA1 region of the hippocampus.[61,62] LTP triggers a persistent activation of CaMKII via the formation of CaMKII-GluN2B complexes, which promotes the delivery of new functional GluA1-expressing AMPA receptors to synapses.[40,54,63–65] Consistently, our data reveal that the increased translocation of active CaMKII to PSD and the post-synaptic enrichment in GluNR-2B upon NMDA and VEGF treatment is associated with membrane insertion and synaptic targeting of GluA1-expressing AMPA receptors. Thus, these results suggest that VEGF signaling might be necessary for LTP in CA1. Although VEGF levels have previously been shown to alter adult hippocampal LTP,[8,19] direct effect of VEGF via its receptor VEGFR2 expressed in neurons has never been established. The findings reported here demonstrate that genetic ablation of VEGFR2 in neural cells or in neurons, as well as its pharmacological inhibition, impaired adult LTP in CA1 but not basal synaptic transmission or presynaptic short-term plasticity. This impairment in LTP induction could result from the unbalanced subunit composition of GluNR at synapses,[66–69] with a decreased content in GluNR-2B due to VEGFR2 deficiency. Our findings extended previous work[6,8] by showing an increase in endogenous VEGF levels upon LTP induction and highlighted the requirement for neuronal VEGFR2 in adult hippocampal LTP, independently of the VEGF impact on neurogenesis and angiogenesis. They further suggest the contribution of VEGFR2 to hippocampal form of learning and memory. Because a causal link between hippocampus-dependent contextual fear memory and a hallmark of LTP has been reported previously,[70] we used a fear-conditioning paradigm to assess the behavioral relevance of VEGFR2. We now demonstrate that targeted deletion of VEGFR2 compromises the formation of fear memory by combining impairment of hippocampus-dependent contextual fear memory with deficits in amygdala-dependent memory. Contribution of VEGF in emotional memory has previously been documented by showing that upregulated and downregulated VEGF levels in the hippocampus improved and impaired performances, respectively, in the passive avoidance task and in contextual fear memory.[6,8] In contrast to our study, these reports used overexpressed soluble VEGFR1[8] or dominant-negative mutant VEGFR2,[6] which produce a VEGF trap and does not give a clear insight into the requirement for VEGFR2 in these cognitive processes. Thus, together with these previous reports, our findings strongly indicate that VEGF and VEGFR2, by acting on different limbic networks, have a key role in the regulation of emotional memory.

Increasing evidence indicate that contextual fear learning requires a network interconnecting the hippocampus, the amygdala and the medial prefrontal cortex,[71–73] whose dysfunction is linked among other disorders to post-traumatic stress disorder and depression.[74–76] In these brain areas, increase in LTP has been shown to result from antidepressant treatments and may be instrumental in the antidepressant response.[77,78] Thus, VEGFR2 dysfunction in these neural networks involved in emotional behavior may attenuate antidepressant response or alternatively promote depression.

In summary, our findings provide new insight into the impact of VEGF on glutamatergic synaptic function and plasticity and further delineate a molecular basis underlying its direct action through VEGFR2 on emotion-related behavior.

CONFLICT OF INTEREST

The authors declare no conflict of interest.

ACKNOWLEDGMENTS

We thank Annabelle Bouchardon and Amandine Durand-Terrasson from the Centre Commun de Quantimétrie (University Lyon 1) and the Microscopy Platform (Grenoble Institut for Neurosciences) for assistance. We are grateful to Carmen Ruiz de Almodovar, Fanny Mann, Alain Buisson and Farida El Gaamouch for helpful discussions. This study was supported by grants from the Institut National de la Santé et de la Recherche Médicale, the Lyon Neuroscience Research Center (to CM) and from the Deutsche Forschungsgemeinschaft (CRC1080) (to AA-P and HJL), EXC 115, EXC147 and SFB 834 (to AA-P), Gutenberg Research College (GRC) (AA-P); PDR and MB were supported by a doctoral research contract from the French Ministry of Higher Education and Research and LM by a doctoral research contract ADR ARC2 from the "Région Rhône-Alpes".

REFERENCES

1 Newton SS, Fournier NM, Duman RS. Vascular growth factors in neuropsychiatry. *Cell Mol Life Sci* 2013; **70**: 1739–1752.
2 Clark-Raymond A, Halaris A. VEGF and depression: a comprehensive assessment of clinical data. *J Psychiatr Res* 2013; **47**: 1080–1087.
3 Warner-Schmidt JL, Duman RS. VEGF is an essential mediator of the neurogenic and behavioral actions of antidepressants. *Proc Natl Acad Sci USA* 2007; **104**: 4647–4652.
4 Greene J, Banasr M, Lee B, Warner-Schmidt J, Duman RS. Vascular endothelial growth factor signaling is required for the behavioral actions of antidepressant treatment: pharmacological and cellular characterization. *Neuropsychopharmacology* 2009; **34**: 2459–2468.
5 Jin K, Zhu Y, Sun Y, Mao XO, Xie L, Greenberg DA. Vascular endothelial growth factor (VEGF) stimulates neurogenesis in vitro and in vivo. *Proc Natl Acad Sci USA* 2002; **99**: 11946–11950.
6 Cao L, Jiao X, Zuzga DS, Liu Y, Fong DM, Young D *et al.* VEGF links hippocampal activity with neurogenesis, learning and memory. *Nat Genet* 2004; **36**: 827–835.
7 Schanzer A, Wachs FP, Wilhelm D, Acker T, Cooper-Kuhn C, Beck H *et al.* Direct stimulation of adult neural stem cells in vitro and neurogenesis in vivo by vascular endothelial growth factor. *Brain Pathol* 2004; **14**: 237–248.
8 Licht T, Goshen I, Avital A, Kreisel T, Zubedat S, Eavri R *et al.* Reversible modulations of neuronal plasticity by VEGF. *Proc Natl Acad Sci USA* 2011; **108**: 5081–5086.
9 Udo H, Yoshida Y, Kino T, Ohnuki K, Mizunoya W, Mukuda T *et al.* Enhanced adult neurogenesis and angiogenesis and altered affective behaviors in mice overexpressing vascular endothelial growth factor 120. *J Neurosci* 2008; **28**: 14522–14536.
10 During MJ, Cao L. VEGF, a mediator of the effect of experience on hippocampal neurogenesis. *Curr Alzheimer Res* 2006; **3**: 29–33.
11 Paoletti P, Bellone C, Zhou Q. NMDA receptor subunit diversity: impact on receptor properties, synaptic plasticity and disease. *Nat Rev Neurosci* 2013; **14**: 383–400.
12 Luscher C, Malenka RC. NMDA receptor-dependent long-term potentiation and long-term depression (LTP/LTD). *Cold Spring Harb Perspect Biol* 2012; **4**: a005710.
13 Bliss TV, Collingridge GL. Expression of NMDA receptor-dependent LTP in the hippocampus: bridging the divide. *Mol Brain* 2013; **6**: 5.
14 Abdallah CG, Sanacora G, Duman RS, Krystal JH. Ketamine and rapid-acting antidepressants: a window into a new neurobiology for mood disorder therapeutics. *Annu Rev Med* 2015; **66**: 509–523.

15 Kang HJ, Voleti B, Hajszan T, Rajkowska G, Stockmeier CA, Licznerski P *et al.* Decreased expression of synapse-related genes and loss of synapses in major depressive disorder. *Nat Med* 2012; **18**: 1413–1417.
16 Yuen EY, Wei J, Liu W, Zhong P, Li X, Yan Z. Repeated stress causes cognitive impairment by suppressing glutamate receptor expression and function in prefrontal cortex. *Neuron* 2012; **73**: 962–977.
17 Ruiz de Almodovar C, Coulon C, Salin PA, Knevels E, Chounlamountri N, Poesen K *et al.* Matrix-binding vascular endothelial growth factor (VEGF) isoforms guide granule cell migration in the cerebellum via VEGF receptor Flk1. *J Neurosci* 2010; **30**: 15052–15066.
18 Meissirel C, Ruiz de Almodovar C, Knevels E, Coulon C, Chounlamountri N, Segura I *et al.* VEGF modulates NMDA receptors activity in cerebellar granule cells through Src-family kinases before synapse formation. *Proc Natl Acad Sci USA* 2011; **108**: 13782–13787.
19 Kim BW, Choi M, Kim YS, Park H, Lee HR, Yun CO *et al.* Vascular endothelial growth factor (VEGF) signaling regulates hippocampal neurons by elevation of intracellular calcium and activation of calcium/calmodulin protein kinase II and mammalian target of rapamycin. *Cell Signal* 2008; **20**: 714–725.
20 Duman RS, Aghajanian GK. Synaptic dysfunction in depression: potential therapeutic targets. *Science* 2012; **338**: 68–72.
21 Tronche F, Kellendonk C, Kretz O, Gass P, Anlag K, Orban PC *et al.* Disruption of the glucocorticoid receptor gene in the nervous system results in reduced anxiety. *Nat Genet* 1999; **23**: 99–103.
22 Minichiello L, Korte M, Wolfer D, Kuhn R, Unsicker K, Cestari V *et al.* Essential role for TrkB receptors in hippocampus-mediated learning. *Neuron* 1999; **24**: 401–414.
23 El Gaamouch F, Buisson A, Moustie O, Lemieux M, Labrecque S, Bontempi B *et al.* Interaction between alphaCaMKII and GluN2B controls ERK-dependent plasticity. *J Neurosci* 2012; **32**: 10767–10779.
24 Lee JS, Jang DJ, Lee N, Ko HG, Kim H, Kim YS *et al.* Induction of neuronal vascular endothelial growth factor expression by cAMP in the dentate gyrus of the hippocampus is required for antidepressant-like behaviors. *J Neurosci* 2009; **29**: 8493–8505.
25 Neyton J, Paoletti P. Relating NMDA receptor function to receptor subunit composition: limitations of the pharmacological approach. *J Neurosci* 2006; **26**: 1331–1333.
26 Ivanov A, Pellegrino C, Rama S, Dumalska I, Salyha Y, Ben-Ari Y *et al.* Opposing role of synaptic and extrasynaptic NMDA receptors in regulation of the extracellular signal-regulated kinases (ERK) activity in cultured rat hippocampal neurons. *J Physiol* 2006; **572**: 789–798.
27 Bard L, Groc L. Glutamate receptor dynamics and protein interaction: lessons from the NMDA receptor. *Mol Cell Neurosci* 2011; **48**: 298–307.
28 Groc L, Choquet D. Measurement and characteristics of neurotransmitter receptor surface trafficking (Review). *Mol Membr Biol* 2008; **25**: 344–352.
29 Coultrap SJ, Bayer KU. CaMKII regulation in information processing and storage. *Trends Neurosci* 2012; **35**: 607–618.
30 Sanz-Clemente A, Gray JA, Ogilvie KA, Nicoll RA, Roche KW. Activated CaMKII couples GluN2B and casein kinase 2 to control synaptic NMDA receptors. *Cell Rep* 2013; **3**: 607–614.
31 Dupuis JP, Ladepeche L, Seth H, Bard L, Varela J, Mikasova L *et al.* Surface dynamics of GluN2B-NMDA receptors controls plasticity of maturing glutamate synapses. *EMBO J* 2014; **33**: 842–861.
32 Strack S, Colbran RJ. Autophosphorylation-dependent targeting of calcium/calmodulin-dependent protein kinase II by the NR2B subunit of the N-methyl-D-aspartate receptor. *J Biol Chem* 1998; **273**: 20689–20692.
33 Lan JY, Skeberdis VA, Jover T, Grooms SY, Lin Y, Araneda RC *et al.* Protein kinase C modulates NMDA receptor trafficking and gating. *Nat Neurosci* 2001; **4**: 382–390.
34 Lau CG, Takayasu Y, Rodenas-Ruano A, Paternain AV, Lerma J, Bennett MV *et al.* SNAP-25 is a target of protein kinase C phosphorylation critical to NMDA receptor trafficking. *J Neurosci* 2010; **30**: 242–254.
35 Yan JZ, Xu Z, Ren SQ, Hu B, Yao W, Wang SH *et al.* Protein kinase C promotes N-methyl-D-aspartate (NMDA) receptor trafficking by indirectly triggering calcium/calmodulin-dependent protein kinase II (CaMKII) autophosphorylation. *J Biol Chem* 2011; **286**: 25187–25200.
36 Newton AC. Protein kinase C: structural and spatial regulation by phosphorylation, cofactors, and macromolecular interactions. *Chem Rev* 2001; **101**: 2353–2364.
37 Zhu JJ, Malinow R. Acute versus chronic NMDA receptor blockade and synaptic AMPA receptor delivery. *Nat Neurosci* 2002; **5**: 513–514.
38 Boehm J, Kang MG, Johnson RC, Esteban J, Huganir RL, Malinow R. Synaptic incorporation of AMPA receptors during LTP is controlled by a PKC phosphorylation site on GluR1. *Neuron* 2006; **51**: 213–225.
39 Opazo P, Labrecque S, Tigaret CM, Frouin A, Wiseman PW, De Koninck P *et al.* CaMKII triggers the diffusional trapping of surface AMPARs through phosphorylation of stargazin. *Neuron* 2010; **67**: 239–252.
40 Malinow R, Malenka RC. AMPA receptor trafficking and synaptic plasticity. *Annu Rev Neurosci* 2002; **25**: 103–126.
41 Faehling M, Koch ED, Raithel J, Trischler G, Waltenberger J. Vascular endothelial growth factor-A activates Ca2+ -activated K+ channels in human endothelial cells in culture. *Int J Biochem Cell Biol* 2001; **33**: 337–346.
42 Cheng HW, James AF, Foster RR, Hancox JC, Bates DO. VEGF activates receptor-operated cation channels in human microvascular endothelial cells. *Arterioscler Thromb Vasc Biol* 2006; **26**: 1768–1776.
43 Xu JY, Zheng P, Shen DH, Yang SZ, Zhang LM, Huang YL *et al.* Vascular endothelial growth factor inhibits outward delayed-rectifier potassium currents in acutely isolated hippocampal neurons. *Neuroscience* 2003; **118**: 59–67.
44 Sun GC, Ma YY. Vascular endothelial growth factor modulates voltage-gated Na(+) channel properties and depresses action potential firing in cultured rat hippocampal neurons. *Biol Pharm Bull* 2013; **36**: 548–555.
45 McCloskey DP, Croll SD, Scharfman HE. Depression of synaptic transmission by vascular endothelial growth factor in adult rat hippocampus and evidence for increased efficacy after chronic seizures. *J Neurosci* 2005; **25**: 8889–8897.
46 Cammalleri M, Martini D, Ristori C, Timperio AM, Bagnoli P. Vascular endothelial growth factor up-regulation in the mouse hippocampus and its role in the control of epileptiform activity. *Eur J Neurosci* 2011; **33**: 482–498.
47 Wittko-Schneider IM, Schneider FT, Plate KH. Brain homeostasis: VEGF receptor 1 and 2-two unequal brothers in mind. *Cell Mol Life Sci* 2013; **70**: 1705–1725.
48 Sahay A, Kim CH, Sepkuty JP, Cho E, Huganir RL, Ginty DD *et al.* Secreted semaphorins modulate synaptic transmission in the adult hippocampus. *J Neurosci* 2005; **25**: 3613–3620.
49 Bouzioukh F, Daoudal G, Falk J, Debanne D, Rougon G, Castellani V. Semaphorin3A regulates synaptic function of differentiated hippocampal neurons. *Eur J Neurosci* 2006; **23**: 2247–2254.
50 Tran TS, Rubio ME, Clem RL, Johnson D, Case L, Tessier-Lavigne M *et al.* Secreted semaphorins control spine distribution and morphogenesis in the postnatal CNS. *Nature* 2009; **462**: 1065–1069.
51 Arrigoni E, Greene RW. Schaffer collateral and perforant path inputs activate different subtypes of NMDA receptors on the same CA1 pyramidal cell. *Br J Pharmacol* 2004; **142**: 317–322.
52 Groc L, Heine M, Cousins SL, Stephenson FA, Lounis B, Cognet L *et al.* NMDA receptor surface mobility depends on NR2A-2B subunits. *Proc Natl Acad Sci USA* 2006; **103**: 18769–18774.
53 Lau CG, Zukin RS. NMDA receptor trafficking in synaptic plasticity and neuropsychiatric disorders. *Nat Rev Neurosci* 2007; **8**: 413–426.
54 Barria A, Malinow R. NMDA receptor subunit composition controls synaptic plasticity by regulating binding to CaMKII. *Neuron* 2005; **48**: 289–301.
55 Gambrill AC, Barria A. NMDA receptor subunit composition controls synaptogenesis and synapse stabilization. *Proc Natl Acad Sci USA* 2011; **108**: 5855–5860.
56 Wang CC, Held RG, Chang SC, Yang L, Delpire E, Ghosh A *et al.* A critical role for GluN2B-containing NMDA receptors in cortical development and function. *Neuron* 2011; **72**: 789–805.
57 Cui Z, Feng R, Jacobs S, Duan Y, Wang H, Cao X *et al.* Increased NR2A:NR2B ratio compresses long-term depression range and constrains long-term memory. *Sci Rep* 2013; **3**: 1036.
58 Barria A, Malinow R. Subunit-specific NMDA receptor trafficking to synapses. *Neuron* 2002; **35**: 345–353.
59 Tovar KR, Westbrook GL. Mobile NMDA receptors at hippocampal synapses. *Neuron* 2002; **34**: 255–264.
60 Bellone C, Nicoll RA. Rapid bidirectional switching of synaptic NMDA receptors. *Neuron* 2007; **55**: 779–785.
61 Citri A, Malenka RC. Synaptic plasticity: multiple forms, functions, and mechanisms. *Neuropsychopharmacology* 2008; **33**: 18–41.
62 Nicoll RA, Roche KW. Long-term potentiation: peeling the onion. *Neuropharmacology* 2013; **74**: 18–22.
63 Lisman J, Yasuda R, Raghavachari S. Mechanisms of CaMKII action in long-term potentiation. *Nat Rev Neurosci* 2012; **13**: 169–182.
64 Bredt DS, Nicoll RA. AMPA receptor trafficking at excitatory synapses. *Neuron* 2003; **40**: 361–379.
65 Lu W, Isozaki K, Roche KW, Nicoll RA. Synaptic targeting of AMPA receptors is regulated by a CaMKII site in the first intracellular loop of GluA1. *Proc Natl Acad Sci USA* 2010; **107**: 22266–22271.
66 Tang YP, Shimizu E, Dube GR, Rampon C, Kerchner GA, Zhuo M *et al.* Genetic enhancement of learning and memory in mice. *Nature* 1999; **401**: 63–69.
67 Gardoni F, Mauceri D, Malinverno M, Polli F, Costa C, Tozzi A *et al.* Decreased NR2B subunit synaptic levels cause impaired long-term potentiation but not long-term depression. *J Neurosci* 2009; **29**: 669–677.
68 Brigman JL, Wright T, Talani G, Prasad-Mulcare S, Jinde S, Seabold GK *et al.* Loss of GluN2B-containing NMDA receptors in CA1 hippocampus and cortex impairs long-term depression, reduces dendritic spine density, and disrupts learning. *J Neurosci* 2010; **30**: 4590–4600.

69 Shipton OA, Paulsen O. GluN2A and GluN2B subunit-containing NMDA receptors in hippocampal plasticity. *Philos Trans R Soc Lond B Biol Sci* 2014; **369**: 20130163.
70 Matsuo N, Reijmers L, Mayford M. Spine-type-specific recruitment of newly synthesized AMPA receptors with learning. *Science* 2008; **319**: 1104–1107.
71 Maren S, Phan KL, Liberzon I. The contextual brain: implications for fear conditioning, extinction and psychopathology. *Nat Rev Neurosci* 2013; **14**: 417–428.
72 Zelikowsky M, Hersman S, Chawla MK, Barnes CA, Fanselow MS. Neuronal ensembles in amygdala, hippocampus, and prefrontal cortex track differential components of contextual fear. *J Neurosci* 2014; **34**: 8462–8466.
73 Gilmartin MR, Balderston NL, Helmstetter FJ. Prefrontal cortical regulation of fear learning. *Trends Neurosci* 2014; **37**: 455–464.
74 Shin LM, Liberzon I. The neurocircuitry of fear, stress, and anxiety disorders. *Neuropsychopharmacology* 2010; **35**: 169–191.
75 Sotres-Bayon F, Sierra-Mercado D, Pardilla-Delgado E, Quirk GJ. Gating of fear in prelimbic cortex by hippocampal and amygdala inputs. *Neuron* 2012; **76**: 804–812.
76 Pitman RK, Rasmusson AM, Koenen KC, Shin LM, Orr SP, Gilbertson MW *et al.* Biological studies of post-traumatic stress disorder. *Nat Rev Neurosci* 2012; **13**: 769–787.
77 Wang JW, David DJ, Monckton JE, Battaglia F, Hen R. Chronic fluoxetine stimulates maturation and synaptic plasticity of adult-born hippocampal granule cells. *J Neurosci* 2008; **28**: 1374–1384.
78 Karpova NN, Pickenhagen A, Lindholm J, Tiraboschi E, Kulesskaya N, Agustsdottir A *et al.* Fear erasure in mice requires synergy between antidepressant drugs and extinction training. *Science* 2011; **334**: 1731–1734.

Supplementary Information accompanies the paper on the Molecular Psychiatry website (http://www.nature.com/mp)